Mechanistic and Structural Features of Protein Adsorption onto Mesoporous Silicates

Joseph Deere, Edmond Magner,* J. Gerard Wall, and B. Kieran Hodnett

Materials and Surface Science Institute and Department of Chemical and Environmental Sciences, University of Limerick, Limerick, Ireland

Received: October 25, 2001; In Final Form: February 25, 2002

The adsorption of cytochrome c onto a range of different mesoporous silicates (MPS) was studied. The materials used, templated using both cationic and nonionic surfactants, have average pore-size diameters in the range from 28 to 130 Å. Cytochrome c was found to bind to all MPS investigated, with the pore diameter of the material, which was measured by N_2 gas adsorption, being crucial to mesopore penetration. The adsorption of a range of proteins with isoelectric points between 1 and 10 was investigated. For adsorption to occur, the surface charges of the protein and of the MPS must be complementary, in addition to the requirement that the pore diameter be sufficiently large. Pepsin at pH 6.5, for example, is negatively charged and does not adsorb onto cyano-modified silicate whereas subtilisin, which is of a similar size and bears an overall positive charge, is adsorbed. Using resonance Raman spectroscopy, cytochrome c was observed to occur in both high spin and low spin states, in contrast to that in solution, where the protein is predominantly in the low spin state. The presence of the high spin state may account for the enhanced peroxidative activity of the adsorbed protein.

Introduction

Mesoporous silicates (MPS) have been the subject of much interest since they were first described by Beck et al. in 1992[1]. MPS possess large surface areas (up to 1000 $m^2\ g^{-1}$), highly ordered pore structures and very tight pore size distributions (PSD); properties which have made these materials attractive candidates for a wide range of applications in catalysis,[2,3] sensor,[4,5] and separation technologies.[6,7] These materials have pore channels of diameter 1.5 to 10 nm which are of a similar size range to small proteins, and in particular, globular proteins. MPS possess a number of additional attributes, which make them attractive candidates for the immobilization of proteins. It is possible to chemically modify their surfaces with various functional groups, enabling electrostatic attraction or repulsion between an MPS and the biological molecule of interest to be maximized.[8] As a result of their silicate inorganic framework, MPS are chemically and mechanically stable and are resistant to microbial attack. Materials such as sol−gels display similar stability to MPS and have been used to encapsulate proteins for use as biosensors.[9,10] However, sol−gels suffer from the disadvantage of possessing a highly variable pore size distribution (PSD). More importantly, their preparation can involve the use of harsh conditions or reagents, which are detrimental to, and can cause denaturation of proteins.[11] Using MPS, protein encapsulation occurs after synthesis of the support, avoiding this difficulty. MPS therefore hold great promise for use as supports to immobilize enzymes and may find applications in biosensors,[12] biocatalytic[13] and biomolecule separation systems.[8]

Protein adsorption/immobilization onto silicate and other inorganic matrixes has been reviewed by Weetall[14] and numerous studies of protein adsorption onto silicate surfaces are to be found in the literature.[15−17] In the 1970s, Weetall et al. pioneered the use of porous inorganic materials for the immobilization of biological molecules and in particular the use of controlled pore glass (CPG).[18−23] CPG materials of pore sizes ranging from 300 to 2000 Å have frequently been reported in such studies, and generally, it has been found that the pore size of the CPG needs to be significantly larger than the biomolecule of interest. For instance, the activity of amyloglucosidase sharply decreased when the CPG pore size was less than 300 Å, and maximal activity was reported for a pore size of 400 Å. The enzyme loading was a direct consequence of both the pore size of the CPG and its surface area, with maximal activity occurring with material possessing both an optimal pore size and an optimal surface area.[19] The major disadvantages in using such materials are their cost and more importantly their surface area, which rapidly decreases with increasing pore size.[19,23]

There have been a number of reports describing the use of MPS to immobilize proteins.[8,12,13,24−30] Balkus et al.[12,24] have immobilized cytochrome c (cyt c), papain, and trypsin onto MCM-41, SBA-15, and layered niobium oxide NB-TMS4. They have shown, as have Stucky et al.;[8] that the adsorption of proteins is dependent on the pore size of the material with, for example, adsorption of peroxidase onto MCM-41 being restricted due to the pore sizes being smaller than the enzyme.[24] Values of pH less than 7.0 were found to favor adsorption of papain and trypsin on MCM-41, whereas for cyt c, adsorption was most efficient at pH greater than 7.0. Desorption of papain occurred above pH 9.0, whereas no cyt c was desorbed at this pH. Cyt c immobilized onto MPS was stable under what would normally be denaturing conditions, and remained electrochemically active for several months.[12] Penicillin acylase (PA) has been adsorbed on to MCM-41 and also by cross linking to silylated MCM-41 using glutaraldeyde as the cross linking agent. The activity of the adsorbed PA was more than five times that of the cross linked enzyme.[25] We have recently shown, by generating adsorption isotherms for cyt c on to a range of MPS, that adsorption is dependent on the silicate pore size and that the peroxidative activity of the adsorbed protein is higher than that of the aqueous protein.[13]

Takahashi et al., investigated the immobilization of horseradish peroxidase (HRP) and subtilisin on to FSM-16 (folded sheet mesoporous material), MCM-41 (both synthesized using cationic

* To whom correspondence should be addressed. Fax: +353-61-202568. Tel: +353-61-202629. E-mail: edmond.magner@ul.ie.

10.1021/jp0139484 CCC: $22.00
Published on Web 06/27/2002

surfactants), and SBA-15 (synthesized using a nonionic surfactant).[29] No significant adsorption of either protein was detected onto SBA-15, despite the large pore size diameter of the latter. This was attributed to the presence of a higher number of negatively charged groups on the surface of FSM-16/MCM-41 resulting in a larger adsorption capacity for cationic proteins compared to a silicate synthesized using nonionic surfactants such as SBA-15. For example, the amounts of HRP and of subtilisin adsorbed onto FSM-16 were 183 and 198 mg (g MPS)$^{-1}$, respectively, whereas with an SBA-15 material of similar pore size only 24 and 28 mg (g MPS)$^{-1}$, respectively, were adsorbed.

Yiu et al., have shown that trypsin adsorbed onto MCM-41, MCM-48, and SBA-15 hydrolyses peptides, but considerable desorption was detected from MCM-48 (72%).[27] SBA-15 supported trypsin showed a higher activity than trypsin adsorbed on to the smaller pore MCM-41. Trypsin supported porous silica gel was found to possess a higher activity than any of the MPS supported preparations. This was explained by the larger proportion of enzyme adsorbed on the outer surface area of the porous silica gel compared to the MPS. Other studies using SBA-15 functionalized surfaces have shown that the tailoring of MPS surface functional groups is extremely important in enhancing the interactions of the protein surfaces and the MPS surface.[28] For trypsin, thiol, chloride, and carboxylic moieties on the MPS surface produced a more stable, adsorbed protein. The presence of phenyl and amine groups on the surface of MPS led to considerable desorption of supported trypsin (19−25%); these values were considerably less (48−52%) than the amounts desorbed from unfunctionalized SBA-15.

In this paper, the interactions of cyt c with a range of MPS materials are examined in detail. Cyt c is an alkaline heme containing redox protein of relatively small size (unit cell size $a = b = 58.34$ Å, $c = 41.83$ Å, molecular mass of 12 384 D)[31−33] which has been the subject of immense biological investigation. A wealth of structural/spectroscopic data[31−37] exists on cytochrome c, making it an ideal candidate for the study of the interactions between MPS and a protein. The environment of the heme group of adsorbed cytochrome c can be selectively probed using Resonance Raman spectroscopy, whereas the effects of isoelectric point (IEP), ionic strength and pH are used to examine the nature of the interactions between the protein and the silicate. Nitrogen adsorption/desorption data of MPS materials before and after adsorption are used to demonstrate the extent of pore filling with protein.

Experimental Section

Reagents. Cetyltrimethylammonium bromide (CTAB, 99%), horse heart cyt c (90% pure), α-chymotrypsin (bovine pancreas) (90% pure), pepsin (bovine stomach) (80% pure), horseradish peroxidase (HRP, 95% pure), glucose oxidase (GOx, *Aspergillus niger*, 95% pure), myoglobin (horse heart, 95% pure), subtilisin Carlsberg VIII (*Bacillus licheniformis*, 95% pure), trypsin (bovine pancreas, 95% pure), bovine serum albumin (95% pure), ammonia (37% w/v), poly(ethylene glycol) (PEG, average molecular weight 1000 Da), ammonium sulfate and potassium phosphate buffer were obtained from Sigma-Aldrich. Oxidized cyt c was purified using established procedures.[38] All other proteins were used without further purification. Commercial kieselgel silica (COS) was obtained from Fluka (Reidal de Häen, product number 31 607). Tetraethoxysilane (TEOS, 98%) and 2-cyanoethyltriethoxysilane (CEOS, 98%) were purchased from Lancaster. Pluronic-F127 ($EO_{106}PO_{70}EO_{106}$) and Pluronic-P123 ($EO_{20}PO_{70}EO_{20}$) were obtained as a gift from BASF. Water was purified (18.2 MΩ) using an Elgastat SPECTRUM system.

Synthesis and Characterization of MPS Materials. MPS with cyano-functional groups (CNS) was synthesized by mixing 50 g CTAB with 450 g of H_2O. This solution was heated to 30 °C until all of the surfactant was dissolved, after which 50 mL TEOS, 6.25 mL CEOS, and 2.5 mL NH_3 were added. The gel mixture was heated to 105 °C for 24 h. The surfactant was removed by refluxing in a methanol solution containing 1.5% HCl and 2.5% H_2O. The CNS material was refluxed until no change in mass was observed. CNS−Cal was formed by calcination of CNS (ramp rate 1 °C min^{-1}) and held at 650 °C for 6 h under a stream of air (100 cm^3 min^{-1}). MCM-41 was synthesized by mixing 10 g CTAB, 1 g NaOH, and 90 g H_2O at 35 °C. On dissolution of the surfactant, 9 mL of TEOS and 2.5 mL of CEOS were added and stirred at 35 °C for 30 min. The mixture was then heated to 150 °C for 24 h. The solid product was filtered and added to 200 mL H_2O, followed by stirring and heating to 70 °C for 10 min. The surfactant was removed by calcination at 650 °C for 6 h (ramp rate of 1 °C min^{-1}). MPS−F127 was synthesized using the nonionic tri-block copolymer Pluronic-F127 as the structure directing agent.[39] The silicate was prepared by stirring 1 g of Pluronic-F127, 7.5 g H_2O, and 30 g of 2 M HCl at room temperature. On dissolution of the surfactant, 2.28 mL of TEOS was added and the solution stirred for 24 h at room temperature. The gel was aged at 100 °C for 20 h and filtered/washed with methanol and pure water (500 mL, 3:1 (w/w)). The washed product was calcined at 500 °C for 6 h (ramp rate of 1 °C min^{-1}).

All of the silicates used were characterized by nitrogen gas adsorption/desorption isotherms at 77 K measured using a Micromeritics Gemini ASAP 2000 system. Samples were pretreated by heating at 150 °C for 1 h. The pore size data were analyzed by the thermodynamic based Barrett−Joyner−Halenda (BJH) method[40] using the desorption branch of the isotherm and surface areas were measured using the Brunauer−Emmett−Teller (BET) method.[41]

Protein Adsorption. Protein adsorption isotherms for the different proteins were generated by contacting protein (0.1−40 μM) with an MPS suspension (final concentration 1 mg ml^{-1}) in 2.0 mL vials at 25 °C for 16 h. The amount of protein adsorbed was measured by a difference method with protein concentrations determined before and after adsorption by UV absorption at 280 nm (trypsin, $\epsilon_{molar} = 14\,300$ M^{-1} cm^{-1} [42]; subtilisin, $\epsilon_{molar} = 22\,880$ M^{-1} cm^{-1} [43]; bovine serum albumin (BSA), $\epsilon_{molar} = 41\,200$ M^{-1} cm^{-1}; α-chymotrypsin, $\epsilon_{molar} = 41\,500$ M^{-1} cm^{-1}; pepsin, $\epsilon_{molar} = 35\,700$ M^{-1} cm^{-1} and horseradish peroxidase (HRP), $\epsilon_{molar} = 12\,000$ M^{-1} cm^{-1}. Cyt c concentration was determined at 407 nm ($\epsilon_{molar} = 100\,000$ M^{-1} cm^{-1}),[31] glucose oxidase at 450 nm ($\epsilon_{molar} = 14\,100$ M^{-1} cm^{-1})[44] and myoglobin at 418 nm ($\epsilon_{molar} = 120\,000$ M^{-1} cm^{-1}).[45] The effect of ionic strength on the adsorption process was examined using a buffer solution (1 mM phosphate, pH 6.5) with varying concentrations of NaCl.

Nitrogen Gas Adsorption Sample Preparation. Samples of MPS with adsorbed cyt c, which were analyzed by nitrogen gas adsorption, were prepared by stirring gently an MPS suspension (2−10 mg ml^{-1}) with a cyt c solution (10−20 μM) for 16 h. The suspension was then washed with buffer before air drying on filter paper overnight. The sample was then weighed and degassed at room temperature and 5 mbar for 75 min, prior to nitrogen gas adsorption. Samples were not heated during degassing to prevent protein denaturation.[46] Cyt c was removed from the CNS−Cal material (after adsorption) by washing in 10% PEG and 1M $(NH_4)_2SO_4$ (desorbing buffer) for 12 h at 4 °C. This leads to almost complete removal of the

TABLE 1: Physicochemical Features of MPS before and after Cyt c Adsorption

MPS	BET surface area ($m^2\ g^{-1}$)	average pore size (Å)	mesopore volume ($cm^3\ g^{-1}$)	μmol cyt c g^{-1}[a]	volume cyt c adsorbed ($cm^3\ g^{-1}$)[b]
COS	470 [13]	55	0.46[13]	0	0
COS-cyt c	304	59	0.37	0.34 (3.8)	0.0006 (0.0069)
COS-cyt c	82	59	0.10	3.2	0.0056
CNS	377 [13]	130	0.74[13]	0	0
CNS-cyt c	347	121	0.77	0.28 (10.2)	0.0005 (0.0179)
CNS-cyt c	327	120	0.63	3.92	0.0069
CNS−Cal	632	126	0.82	0	0
CNS−Cal-cyt c	423	121	0.63	0.262 (9.5)	0.0005 (0.0167)
CNS−Cal-Des-cyt[c]	405	144	0.78	0.020	0.0000
MCM-41	1,000 [13]	28	0.31[13]	0	0
MCM-41-cyt c	803	23	0.03	0.39 (1.7)	0.0007 (0.0030)
MCM-41-cyt c	595	23	0.04	1.7	0.0030
MPS−F127	537 [13]	50	0.38[13]	0	0
MPS−F127-cyt c	520	31	0.46	0.52 (6.8)	0.0009 (0.0120)
MPS−F127-cyt c	281	34	0.29	1.31	0.0023

[a] The data in brackets refer to the maximum load of cyt c (μmole g^{-1}) achieved for each material. [b] Calculated on the basis of the volume of cyt c molecule 143 nm^3 (from crystal structure data[17(b)]). [c] CNS−Cal−Des−Cyt refers to CNS−Cal material onto which cyt c was adsorbed and then removed.

protein from the CNS−Cal surface (calculated as 94% removal of the original protein loading). The material was then washed extensively (×4) with adsorption buffer (25 mM phosphate, pH 6.5) before air drying.

Zeta Potential Measurements. Isoelectric points were determined using a Malvern Zeta sizer equipped with a titration system (Malvern multipurpose Titrator MPT1). Samples of MPS materials were suspended (~20 mg 100 mL^{-1}) in water (18.2 MΩ) and 50 mL aliquots of these solutions were then titrated with 0.1 M HCl from pH ~8.0 to 2.0. Each titration consisted of 10 points, zeta measurements were determined (in triplicate, s.d. of 5%) at each point and the isoelectric point was calculated using the system software. MPS with adsorbed protein were prepared by gently stirring protein in a 4 mg ml^{-1} MPS suspension (25 mM phosphate at pH 6.5) for 16 h. The MPS−protein was then washed (×4) with water (18.2 MΩ). Protein loss from each wash was accounted for when calculating the protein loading on the MPS. The MPS-protein was then suspended in water and titrated from pH 8.0 to 2.0, as before.

Confocal Resonance Raman Spectroscopy. Confocal Resonance Raman Spectroscopy was carried out using a Jobin Yvon system (LABRAM no 1/168 IM) with excitation at 5145 Å provided by a Uniphase Model 2010 air-cooled argon ion laser. The system was also equipped with an Olympus BX40 microscope (capable of spatially zoning in on 400 $microns^2$ of sample). Samples were prepared in 1.5 mL vials by contacting cyt c (10 μM) with an MPS suspension (1 mg ml^{-1} total MPS concentration (per vial) for 16 h at 25 °C. Samples were centrifuged and the protein loading determined spectrophotometrically. Samples (~1 mg) were suspended in 100 μL of buffer (25 mM phosphate, pH 6.5) and this concentrated solution then pipetted onto a glass slide. The laser was then positioned onto a specific point on a particle in the sample and spectra were generated. All spectra presented have a spectral width of ~9 cm^{-1}, and were generated at a sample magnification of 2000. Spectral peaks were obtained using the system software.

Results and Discussion

Adsorption Studies. The five materials used in these studies exhibit quite different pore sizes and surfaces areas (Table 1). The average pore size and the surface area ranged from 28 (MCM-41) to 144 Å (CNS) and 379 (CNS) to 1000 $m^2\ g^{-1}$ (MCM-41), respectively.[13] MCM-41 alone, possesses an ordered hexagonal structure (Figure 8S). The other silicates are porous

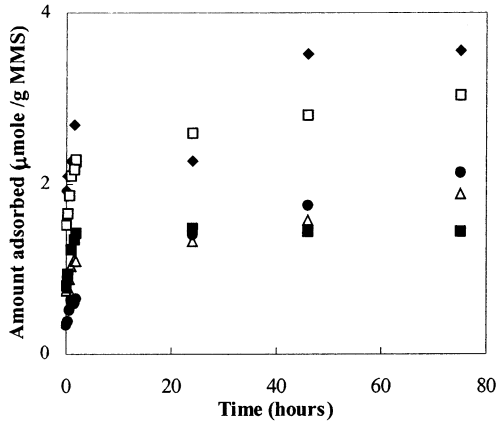

Figure 1. Cyt c adsorption onto CNS(◆), CNS−Cal(□), COS(●), MPS−F127(△), and MCM-41(■) as a function of time; initial cyt c concentration of 7.4 μM.

(Figure 9S) and possess similar particle size distributions (Figure 10S). CNS−Cal exhibited a very similar pore size distribution to CNS. The slight decrease in the pore size of the former can be attributed to contraction of the silica walls on heating.

Cyt c adsorbs readily onto all the MPS materials as has been reported for other protein adsorption systems, e.g., latex beads, (Figure 1).[47] Adsorption is approximately 80% complete after the first 2 h for all five materials. The three smaller pore materials (MCM-41, MPS−F127, and COS) exhibit almost identical adsorption time profiles. Adsorption onto MCM-41[13] can occur only on the external surface (as the pores are too small to allow entry of the protein) and is complete after ~140 min (1.5 μmols g^{-1}). The larger pore materials (CNS, CNS−Cal), whose pore sizes are substantially larger than the protein, exhibit a much higher binding capacity for cyt c.

Desorption. Cyt c adsorbs strongly on MPS. After repeated washings (×5) in adsorption buffer (25 mM phosphate, pH 6.5) no protein was detected in solution. Balkus et al.[48] suggested that the strong adsorption of cyt c onto MPS was dominated by hydrophobic/hydrophilic properties rather than electrostatic interactions. For example at a pH below 10.0 (IEP of cyt c is 10.6[31]) no appreciable amounts of protein were reported to leach out of the lamellar MCM-48 material (~0.3−0.5%), whereas 3−5% was desorbed from the hexagonal MCM-41 material at pH 6.0, 7.0 and 10.0.[48] However, it should be noted that MPS, due to their silica framework, dissolve at pH > 8.0, [49] whereas cyt c is not stable at pH below 3.0 and above 10.0,[31] precluding

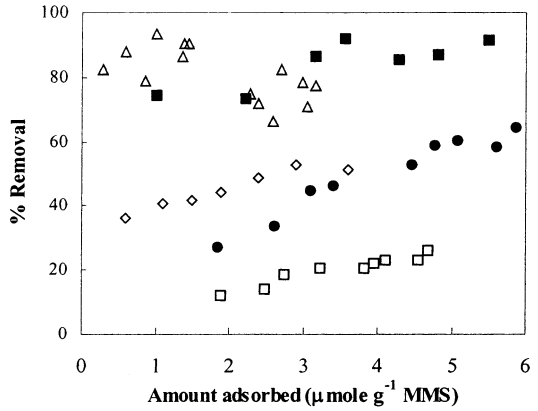

Figure 2. Desorption profiles for cytochrome *c* from COS (10% PEG-(◇), 10% PEG + 1 M $(NH_4)_2SO_4$(◆)), and CNS (10% PEG (□), 1 M $(NH_4)_2SO_4$(●), 10% PEG + 1 M$(NH_4)_2SO_4$(△).

the study of such systems outside the pH range 3−8. The stability of the adsorbed protein was thus investigated by using a range of desorbent materials which could competitively interact with the adsorbed protein on MPS and remove cyt c molecules from the MPS surface.

Poly(ethylene glycol) and 1 M ammonium sulfate ($(NH_4)_2SO_4$) were found to readily desorb the protein from the MPS materials. Figure 2 shows the percentage removal of protein over a range of adsorbed cyt c. Desorption of protein from the CNS material using a buffer containing 10% PEG (w/v) and 1 M $(NH_4)_2SO_4$ was readily achieved with between 75 and 92% of protein being removed from CNS. These desorbents were also investigated individually; 10% PEG was found to desorb 16−30% of the protein whereas 1 M $(NH_4)_2SO_4$ desorbed 28−53% protein over the same adsorbed protein range. Ammonium sulfate therefore desorbs double the amount that PEG achieves, indicating that electrostatic interactions at the CNS-cyt c interface dominate. This is in contrast to the results reported by Balkus et al. for cyt c adsorption onto MCM-41.[24] This difference can be explained by the higher buffer concentration used in that study, 50 mM phosphate, and by the fact that the cytochrome c was not purified, but used as received. As will be discussed below, the ionic strength of the buffer solution influences the degree of electrostatic interactions between cyt c and MPS; in the results reported here, the ionic strength is half of that used previously. Commercially available cytochrome c is 90% pure, with impurities consisting of deamidated and dimeric forms of the protein.[38] Such impurities may interact with MPS in a different manner to the purified protein.

Desorption of cyt c from COS was similarly investigated, with 10% PEG and 1 M $(NH_4)_2SO_4$ together desorbing an identical amount of protein as from CNS. 10% PEG alone (Figure 2) desorbed (38−55%) significantly more (∼double) than from the CNS material suggesting hydrophobic interactions dominate on COS.

The trend of lower amounts of protein being desorbed at lower adsorbed protein levels for the desorbents 1 M $(NH_4)_2SO_4$ and 10% PEG when used individually may indicate that at higher protein loadings on MPS, the protein is either more accessible to the desorbent or, that some multi-protein adsorption layers occur. Desorption of protein molecules from other adsorbed protein molecules may occur more readily than desorption of protein from the MPS surface. The maximum amounts adsorbed for cyt c onto all MPS[13] are approximately equivalent to monolayer coverage. On MCM-41 adsorption occurs only on the surface and not in the pores, indicating that multilayer adsorption does occur. With CNS, the mesopore channels are

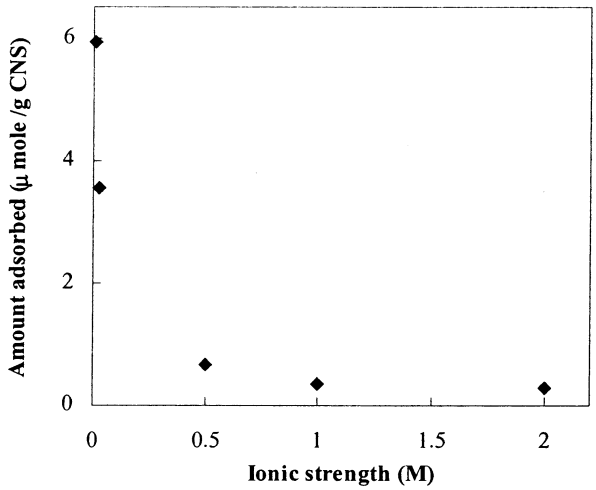

Figure 3. Plot of amount of cyt c adsorbed onto CNS versus inonic strength; solution cyt c concentration of 2 μM.

accessible to cyt c; the theoretical surface coverage by cyt c is equivalent to a monolayer, but as discussed below blockage of some of the channels occurs, indicating that partial multilayer adsorption does occur.

Influence of Ionic Strength. Over the range of ionic strength investigated (Figure 3), the amount of protein adsorbed strongly decreased with increasing ionic strength. The adsorption system used at 25 mM phosphate buffer corresponds to an ionic strength of ca. 50 mM, at which point ∼3.2 μmole cyt c g CNS^{1-} is adsorbed, in agreement with the amount adsorbed in the presence of 50 mM NaCl. When adsorption of cyt c was performed in the presence of 1 M ammonium sulfate, only 0.3 μmole was adsorbed, also in agreement with the data obtained with NaCl. The fact that only 28−53% of cyt c was desorbed from CNS on addition of 1 M ammonium sulfate indicates that adsorption and desorption occur via different pathways and that once the protein is adsorbed, the presence of a high salt concentration is not sufficient to remove the protein from CNS.

Influence of Surface Charged Groups. The ionic strength of the adsorption solution has a profound effect on the levels of cyt c adsorption onto the CNS surface. In analyzing the surface charged species in more detail it is useful to look at zeta potential measurements, from which the IEP can be measured. Such measurements have not, to our knowledge, been previously reported for MPS. The IEP of silica of various forms, from purified ground quartz to colloidal silica, have been reported to be in the range 0.5 to 3.7.[49] MPS−F127 and COS exhibited low IEP values (2.83 ± 0.14 and 2.90 ± 0.15, respectively), whereas MCM-41 and CNS materials had similar, higher IEPs (3.6 ± 0.18 and 3.7 ± 0.22). Takahashi et al.[29] recently observed that larger levels of protein adsorption occurred on MPS templated with cationic surfactants and suggested that this was due to the higher level of negatively charged groups on the surface of these materials compared with MPS templated with nonionic surfactants (i.e., SBA-15[29,39]). These results indicate that the surface charges of MPS as well as those of the protein under the system conditions in use have to be taken into account.

Oxidized cyt c (used throughout these studies) has a net charge of +8 at pH 7.0.[33,39] The surface area of cyt c is ∼55% hydrophobic, despite the presence of a large number of charged species, predominantly lysine and glutamate residues. The lysine residues are mainly found in a cluster around the heme, whereas the negatively charged groups are primarily found on the top and back of the molecule. Thus the charges on cyt c are not

TABLE 2: Isoelectric Point of COS and COS-cyt c

MPS suspension	Cyt c loading (μmole g^{-1})	isoelectric point
COS	0	2.90 ± 0.15
COS	0.12	4.10 ± 0.20
COS-des[a]	0	2.73 ± 0.14
COS	0.34	5.35 ± 0.26
COS-des[a]	0	3.10 ± 0.16

[a] Cytochrome was desorbed using 10% PEG and 1 M $(NH_4)_2SO_4$.

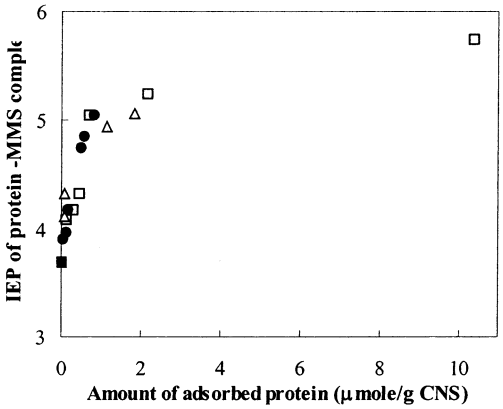

Figure 4. Plot of the isoelectric point (IEP) of protein-NMS complex versus the amount of protein adsorbed on CNS; cytochrome c (□ equilibrium concentration range 2−10 μM), myoglobin (● equilibrium concentration range 2−10 μM), bovine serum albumin (△ equilibrium concentration range 16−78 μM).

symmetrically distributed across the surface of the protein, implying that the protein will adopt a preferred orientation when binding to a charged surface, such as that of MPS. Table 2 presents data on the IEP of COS upon adsorption of cyt c. At cyt c loadings of 0.12 and 0.34 μmol g^{-1}, the isoelectric point increased to 4.10 and 5.35, respectively. On removing the protein from COS (using 10% PEG and 1M $(NH_4)_2SO_4$) the IEP of the material decreased to 2.73 and 3.10, respectively. Although some residual protein may still exist on the surface, these values are very similar to the IEP of 2.90 measured prior to adsorption, and confirm that the increases in IEP are as a result of protein adsorbing onto the COS surface.

The effect of protein adsorption on the IEP of CNS was investigated by measuring its value at different protein loadings. Three different proteins were investigated cyt c (IEP of 10.6),[31] myoglobin (IEP of 7.0),[50] and BSA (IEP of 4.6),[51] spanning the range of IEP values for most proteins. Figure 4 shows the amount of protein adsorbed versus the IEP of each protein−MPS complex. As a control, the degree of retention of the adsorbed proteins on CNS was investigated at pH 3.5, 5.0, 7.0, and 8.0. It was found that no significant leaching occurred for BSA (0−11%) or myoglobin (0.2−11%) from the CNS surface. Similar amounts of cytochrome *c* leached from the surface at pH 8, 7, 5, and 4 (1−9%), whereas at pH 3.5, 77% of the protein leached from the silicate. Thus, over the pH range examined, at least 89% of the protein remained on the MPS material. The large amount of leaching at pH 3.5 is expected because CNS bears an overall positive charge at this pH.

For cyt c, the IEP of the MPS−protein complex increases steadily from that of the initial value obtained with CNS alone (3.7). The highest loading of cyt c (10.6 μmols g^{-1}, the maximum amount that can be adsorbed) gave a value of 5.75. The increase in IEP of the material upon adsorption of cyt c indicates that the relative amount of negative surface charge on the material is decreasing. This can be explained by the protein adsorbing on the surface through the interaction of the positively charged lysine residues on the protein surface with the abundant, negatively charged, silanol groups.[29,33] The adsorption of BSA and myoglobin onto CNS were similarly investigated. With both proteins, a similar steep rise in IEP occurred to ∼5.10, after which no more protein could be adsorbed. These values are lower than IEP obtained with CNS-cyt c which is probably a result of the larger amount of cyt c adsorbed onto CNS. The similarities in isoelectric point of the adsorbed complexes indicates that it is the isoelectric point of the silicate which is being determined, as otherwise dramatically different results would be expected for each system.

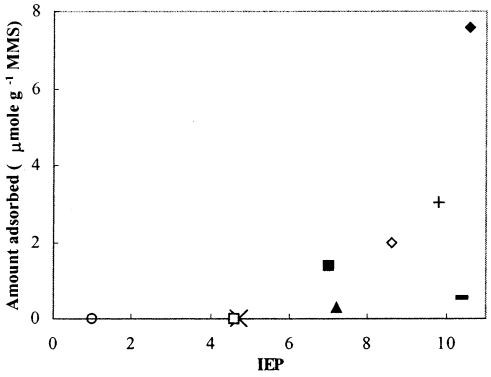

Figure 5. Plot of amount of protein adsorbed on to CNS versus isoelectric point of the protein. Conditions: equilibrium protein concentration of 5 μM, 19 h in 25 mM phosphate buffer at pH 6.5, 25 °C. cytochrome c (12.4 kDa, ◆), subtilisin (30 kDa, -), α-chymotrypsin (23.5 kDa, +), trypsin (◇), horseradish peroxidase (44 kDa, ▲), myoglobin (17.6 kDa, ■), bovine serum albumin (66 kDa, ×), glucose oxidase (160 kDa, □), and pepsin (33 kDa, ○).

The adsorption of a range of different proteins, with different isoelectric points, surface chemistry and sizes was investigated for CNS. Figure 5 presents the amount adsorbed for each protein as a function of the isoelectric point of the protein (all values were determined from individual protein adsorption isotherms at an equilibrium concentration of 5 μM). The amount adsorbed is a function of the IEP of the protein, though not exclusively so. Cyt c exhibits the highest adsorption affinity, whereas no adsorption for pepsin (IEP < 1)[52] or glucose oxidase (GOx, IEP of 4.6)[44] was detected. Pepsin (molecular mass 33 000 D) is much larger than cyt c (12 384 D) but is small enough to fit into the CNS pores (130 Å); however, it possesses an overall negative charge at pH 6.5 preventing adsorption. GOx, has an IEP similar to that of BSA, and is a large protein with an average spherical diameter of 80 Å.[53] Given its size, it should be able to fit into the pores, however its negatively charged surface[54] appears to prevent adsorption on to CNS. Subtilisin, (0.65 μmol g^{-1}) which has a high IEP of 10.4,[43] did not exhibit the high levels of adsorption seen with cyt c. This can be attributed to the larger size of subtilisin, but not solely as CNS adsorbed 2.9 μmol g^{-1} of α-chymotrypsin, a protein of similar size to subtilisin. Subtilisin has a different surface charge topography compared to cyt c, with the surface charges being more evenly distributed.[43] The combination of larger size and different surface charge distribution leads to lower levels of adsorption. These studies show that, for adsorption to occur, it is not sufficient to have a protein of a smaller size than the MPS pore diameters, the IEP and surface charges of the protein and MPS must also be taken into account.

BET Analysis and Pore Characteristics. The effects on pore volume and surface area upon adsorption of cyt c onto MPS were analyzed by nitrogen gas adsorption. Table 1 presents a summary of the physicochemical characteristics of MPS prior to and after cyt c adsorption. With MCM-41 (average pore size

diameter of 28 Å), adsorption of cyt c occurs mainly on the external surface as the protein is too large to penetrate into the channels.[13] When 0.39 μmol cyt c g^{-1} was adsorbed (~25% of the maximum capacity for cyt c) both the surface area and the pore diameter decreased by ca. 20%, whereas the mesopore volume decreased significantly from 0.31 to 0.03 cm^3 g^{-1} MCM-41. These data provide more evidence that cyt c is too large to enter the mesopore networks, and indeed the significant reduction in the mesopore volume points to significant pore blockage at the pore openings upon cyt c adsorption. Because most of the pores are only a few Å smaller than the cyt c molecules, it is reasonable to imagine that protein molecules (depending on their orientation at the pore opening) can partially enter the pores and block them at their openings. This is similar to what Balkus et al.[24] reported for peroxidase (spherical radius of 46 Å) adsorption onto an MCM-41 with a pore diameter of 40 Å where only 0.4 mg peroxidase g^{-1} MCM-41 was adsorbed at pH 6.0, compared to 3.8 mg g^{-1} when cyt c was adsorbed. It would be expected that a material which exhibits such a large pore volume decrease would also exhibit a significant decrease in surface area. For MCM-41, when the maximum amount of cyt c was adsorbed (1.7 μmol g^{-1}), a similar pore volume decrease occurred whereas the surface area only decreased from 1000 to 590 m^2 g^{-1}, indicating that the large sub-population of micropores present are not blocked by cyt c. Due to the relatively larger size of the protein, nitrogen molecules may still adsorb into the channels. It is also reasonable to assume that not all cyt c molecules trapped at the mesopore openings completely block the mesopore openings, allowing limited access to nitrogen molecules. Due to the significant reduction in mesopore volumes (from 0.31 to 0.03 cm^3 g^{-1}) upon adsorption of 0.39 μmol cyt c g^{-1} and the significant surface area (595 m^2 g^{-1}) which exists after maximum adsorption, cyt c molecules appear to preferentially adsorb at the mesopore openings before adsorbing at the micropores.

With COS, adsorption at two different cyt c loadings shows that the mesopore volume and the surface area are significantly reduced at the higher loading of protein (3.2 μmol g^{-1}). This significant reduction in the surface area is a result of tight localized packing of the cyt c molecules in the pore networks. A lower loading (0.34 μmol g^{-1}) resulted in a much smaller decrease in both surface area (from 470 to 304 m^2 g^{-1}) and pore volume (from 0.46 to 0.37 cm^3 g^{-1}), suggesting that either the smaller mesopores are filled first by the protein, or that blockage of the pores occurred. Given that the pore size diameter of COS is not significantly greater than that of cyt c, the latter case is more likely.

Adsorption of cyt c on to CNS did not produce as sharp a decrease in the surface area as with COS. At a similar loading of cyt c (3.92 vs 3.2 μmol g^{-1} on COS), the pore volume decreased by 15% (vs 78% for COS), indicating that the pores were not being blocked to the same extent. Anomalous data were obtained with MPS−F127, with the mesoporous volume undergoing an increase from 0.38 to 0.46 cm^3 g^{-1} upon adsorption of 0.52 μmol of cyt c, whereas the surface area decreased slightly from 537 to 520 m^2 g^{-1}. On increasing the amount of protein to 1.31 μmole, the surface area decreased sharply by 48%, whereas the mesopore volume decreased by 24%. As with COS, the pore size diameter of MPS−F127 is similar to that of cyt c, and it is likely that blockage of the pores is occurring.

It was of interest to remove the protein from the MPS materials after adsorption to examine the effect on the mesopore volume and the surface area. CNS−Cal, which has a mesopore volume of 0.82 cm^3 g^{-1} was prepared with 0.26 μmole cyt c g^{-1}. The mesopore volume of this material was calculated to be 0.63 cm^3 g^{-1}. Cyt c was subsequently removed using 10% PEG and 1M $(NH_4)_2SO_4$. CNS−Cal was found to have a cyt c loading of 0.02 μmols g^{-1} (after desorption) and the mesopore volume reverted to a value close (0.78 cm^3 g^{-1}) to that of the original sample (0.82 cm^3 g^{-1}) (Table 1). The surface area remained virtually unchanged and did not revert back to the value obtained prior to adsorption of cyt c (632 m^2 g^{-1}). This may be attributed to sample preparation (all samples were air-dried overnight and subsequently degassed for 75 min at 5 mbar). Heating, during degassing of CNS with a 3.6 μmole g^{-1} loading of cyt c to 150 °C, resulted in an increase in surface area from 379 to 519 m^2 g^{-1}. This may be due to coke formation on denaturation of the protein and demonstrated that this method of removing water could not be used to give accurate results. To investigate if sample preparation was responsible for the surface area not reverting to its original value, nitrogen gas adsorption was performed on COS which had been treated by stirring in buffer solution overnight, air-dried and degassed as usual. The pore volume did not change, but the surface area was found to have decreased from 470 to 396 m^2 g^{-1}. This decrease was therefore a result of buffer adsorption. The fact that the surface area of the CNS−Cal (upon cyt c removal) did not revert back to the original value of 632 m^2 g^{-1} is due to adsorption of desorbent materials (i.e., buffer, salt, and PEG) onto the surface area and is therefore not a result of sample preparation. An MCM-41 sample with maximum loading of cyt c (1.7 μmol g^{-1}) was degassed for 12 hours[46] and was found to exhibit the same surface area and pore volume as when the sample was degassed for 75 min. Therefore, it was considered that simple air-drying overnight prior to degassing for 75 min would be the most effective and accurate method of preparing samples for nitrogen gas adsorption.

For each MPS material (Table 1), the decrease in mesopore volume calculated by nitrogen gas adsorption was found to be larger than the expected decrease calculated from the volume of cyt c adsorbed. This suggests that, in all of the MPS materials the protein enters a large percentage of the pores and is adsorbed on the surface, but at some stage localized multilayer adsorption takes place leading to pore blockage deep in the pore cavities. Therefore, it is unlikely that complete monolayer coverage of the internal surface area is achieved. The significant surface area reduction (83%) of the COS material on cyt c adsorption can be ascribed to blockage of pores some distance inside the channel network.

Raman Structural Analysis of Adsorbed Cyt c. Cyt c,[31,34,35] other heme proteins,[55] and metalloporphyrin derivatives,[56−58] have been extensively studied over the past three decades using Resonance Raman Spectroscopy (RRS). RRS has also been used to study the interactions of cyt c with other heme proteins (i.e., cytochrome oxidase),[35] membranes,[59] Ag-sol gels[60] and heme derivatives.[61] The presence of in-plane ring modes in such molecules, which are coupled to $\pi-\pi^*$ excitations, allows for strongly enhanced Raman bands to be detected, when such bands are in resonance with any of the dominant electronic transitions.[34,37] These bands have been extensively correlated with particular heme vibrational modes. It has been shown, for example, that bands above 1300 cm^{-1} correlate with structural parameters of the heme environment such as oxidation and spin state as well as the coordination numbers of the heme iron.[37] Bands from 1000 to 1700 cm^{-1} have been correlated with C_b-C_b, C_a-C_m, C_a-N bonds of the porphyrin structure.[35−37] The lower frequency bands below 1000 cm^{-1} (which are also less

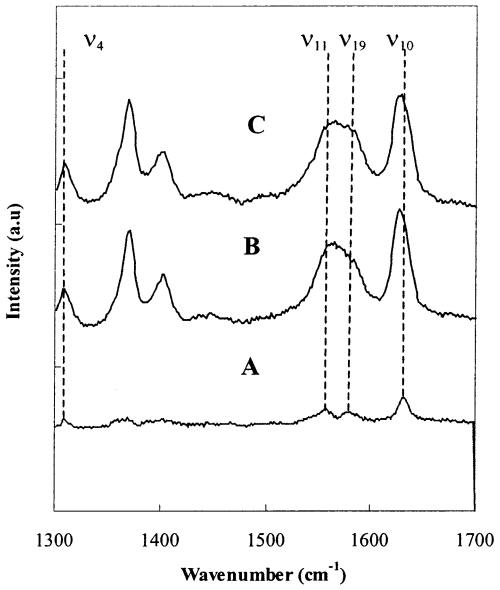

Figure 6. Resonance Raman spectra of aqueous cyt c (A, 1 mM) and of cyt c adsorbed onto COS (B, 2.3 μmol g^{-1}) CNS (C, 1.4 μmol g^{-1}).

intense compared to the higher frequency bands) have been correlated to deformation modes and the bending of the propionate and other substituents attached to C_b.[62] The weaker nature of such bands have been attributed to their greater distance from the $\pi-\pi^*$ excitations.[36] RRS is a more informative structural probe for heme proteins than FT-IR,[63] as it provides detailed information (primarily regarding the proteins heme environment) not possible to obtain using FT-IR which is used to determine the global α-helical and β-sheet content of proteins. We previously reported on the peroxidative activity of cyt c^{3+} which was adsorbed onto MPS. The activity of the adsorbed protein was found to be higher than that of the aqueous protein,[13] indicating that some structural change(s) to the protein may have occurred. Resonance Raman Spectroscopy was used to probe the heme environment for changes in the structure of the protein upon adsorption.

The prominent vibrational bands in RR spectra of aqueous cyt c^{3+} excited at 514 nm are a result of a vibronic coupling mechanism (B term).[34] These refer largely to nontotally symmetric vibrations, the most distinct of which are the spin-state marker bands ν_{11}, ν_{19}, and ν_{10}.[37] Spectra for all MPS materials prior to adsorption exhibited no peaks, after adsorption of cyt c^{3+} onto all MPS materials, spectra were readily generated (depending on the cyt c loading) which exhibited characteristic RR bands for cyt c^{3+}. Spectra for CNS with cyt c^{3+} adsorbed are presented in Figure 6. As expected from the protein loadings used, the spectra obtained with adsorbed protein are significantly more intense than the spectrum of the aqueous protein. The most prominent peaks, as expected from the excitation line (514 nm), are ν_{11}, ν_{19}, and ν_{10}, but surprisingly the ν_4 band in all spectra is also quite prominent.

Table 3 summarizes the major bands of cyt c^{3+} upon adsorption on to the five MPS materials. The spin state marker bands ν_{10}, ν_{11}, ν_{19}, indicate that the Fe heme exists in both the high (HS) and low spin (LS) states at the MPS surface. For example, cyt c (Fe^{3+}) adsorbed onto Ag sol has been reported to exhibit RR bands at 1583 and 1635 cm^{-1} and SERS bands for HS at 1568 and 1626 cm^{-1} for ν_{10} and ν_{19}, respectively.[37] The ν_{10} bands of all the MPS-cyt c^{3+} are close to the 1626 cm^{-1} HS marker band (i.e., 1623, 1620, 1628, 1630, and 1618 cm^{-1}) but the ν_{19} band suggests that the low spin state is also prominent at the MPS surface (especially for CNS, MPS−F127,

TABLE 3: Band Assignments of Resonance Raman Spectra of Cyt c Adsorbed onto MPS

peak assignment (cm^{-1})	aqueous cyt c ref 22	aqueous cyt c this work	cyt c adsorbed COS	CNS	CNS−Cal	MPS−F127	MCM-41
ν_{10}	1634	1632	1623	1620	1628	1618	1630
ν_{19}	1584	1578	1577	1580	1571	1583	1578
ν_{11}	1561	1558	1536	1536	1555	1541	1558
ν_4	1373	1361	1355	1358	1366	1360	1366

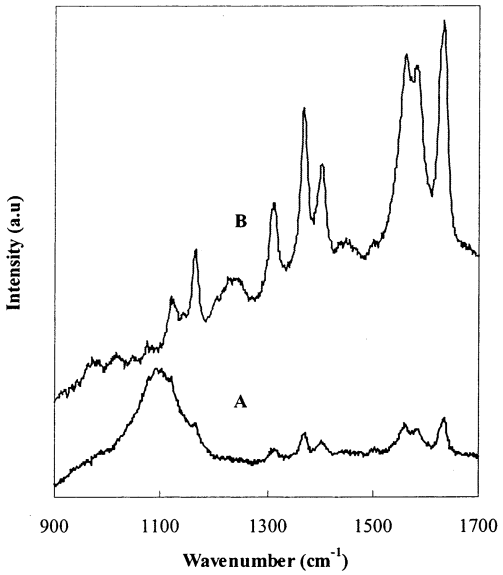

Figure 7. Resonance Raman spectra of MCM-41-cyt c at a protein loading of 1.7 μM. Spectra A and B were obtained on 80% and 20% of sampled positions, respectively.

and MCM-41). At room temperature, aqueous cyt c^{3+} is largely in a LS state.[64] The unexpected prominence of the depolarized ν_4 band in all spectra has also been attributed to the depopulation of the LS state in favor of the HS state.[37] The increased activity of adsorbed cyt c^{3+}, particularly that observed with MCM-41-cyt c^{3+}, may be a result of these significantly higher levels of high spin Fe^{3+}.

The spectra collected at different positions on the same particle of sample are similar, suggesting that any distortions in the heme environment are of a similar nature. The differences in band intensities can be attributed to localized differences in the cyt c^{3+} concentration at the MPS surfaces. The different orientations of the molecules at the surface and their interactions, both with each other and the surface may also contribute to these different intensities.

The MCM-41 (Figure 7) sample exhibited two different populations of spectra. The spectra generated on ~80% (i.e., this value was obtained from 5 different spectra at different points on four separately prepared samples) of positions of MCM-41-cyt c^{3+} particles exhibited a broad band at 1100 cm^{-1}, the intensity of which was greater than the other prominent bands (namely, ν_4, ν_{10}, ν_{19}). As cyt c^{3+} is adsorbed only on the outer surface of this material, the two different spectral patterns appear to be due to cytochrome *c* adsorbed on the surface (20%), and to protein present in the multiple layers (80%). This was confirmed by examining the spectrum of MCM-41-cyt c where the protein loading was reduced from 1.7 to 0.8 μmol g^{-1}. The relative intensity of the band at 1100 cm^{-1} to the intensities at ν_4, ν_{10}, and ν_{19} was reduced. Bands at 1100 cm^{-1} for Q_1 excitation have been attributed largely to C_a-N and C_b-ethyl anti-symmetric stretching with respect to the C_2-axis of a pyrrole ring

in nickel octaethylporphyrin.[65] This band has not been previously reported for cytochrome c; it appears to be indicative of multiply adsorbed layers of the protein. The absence of the broad band at 1100 cm^{-1} for the other materials then suggests that, at the concentrations examined, little multilayer adsorption occurs.

Conclusions

Cytochrome *c* has a high affinity for MPS materials templated with both cationic and nonionic surfactants. The dimensions of the pores of the MPS are crucial for adsorption into the mesopore networks. Cytochrome c is a small, compact protein with a high IEP, properties necessary for adsorption on to MPS. Desorption of the protein in the presence of ammonium sulfate indicates that electrostatic interactions are predominant with CNS, whereas hydrophobic interactions are more predominant with the more positively charged COS. From the BET analysis, cyt c penetrates deep into the mesopore network, when the diameter of the mesopores is larger than that of the protein. Using a range of proteins, it was shown that adsorption of protein on to MPS requires that the surface charges of MPS and the protein be compatible. For example, pepsin, which is negatively charged, does not adsorb onto CNS, whereas subtilisin, which is of a similar size, but positively charged, is adsorbed. From Resonance Raman spectra, cyt c (Fe^{3+}) exists in both high and low spins states, in contrast to the predominantly low spin state form in solution. The presence of significantly higher levels of cyt c with the Fe heme in the high spin state may explain the higher peroxidative activity of the adsorbed protein.

Acknowledgment. This research was funded by the Higher Education Authority through the Program for Research in Third Level Institutions (1999-2000). BASF are thanked for the gift of pluronics.

Supporting Information Available: XRD and TEM data for MCM-41 and CNS respectively and particle size data for each MPS (3 figures). This information is available free of charge via the Internet at http://pubs.acs.org.

References and Notes

(1) Beck, J. S.; Vartuli, J. C.; Roth, W. J.; Leonowicz, M. E.; Kresge, C. T.; Schmitt, K. D.; Chu, C. T.; Olson, D. H.; Sheppard, E. W.; McCullen, S. B.; Higgins, J. B.; Schlenker, J. L. *J. Am. Chem. Soc.* **1992**, *114*, 10 834.
(2) Johnson, B. F. G.; Raynor, S. A.; Shephard, D. S.; Mashmeyer, T.; Thomas, J. M.; Sankar, G.; Bromley, S.; Oldroyal, R.; Gladden, L.; Mantle, M. D. *Chem. Commun.* **1999**, 1167.
(3) Zhang, Z.; Suo, J.; Zhang, X.; Li, S. *Chem. Commun.* **1998**, 241.
(4) Chakraborty, P. *J. Mater. Sci.* **1998**, *33*, 2235.
(5) Yang, P.; Wirnsberger, H. C.; Huang, S. R.; Cordero, M. D.; McGehee, B. S.; Deng, T.; Whitesides, G. M.; Chmelka, B. F.; Buratto, S. K.; Stucky G. D. *Science*. **2000**, *287*, 465.
(6) Vartuli, J. C.; Shih, S. S.; Kresge, C. T.; Beck, J. S. *Stud. Surf. Sci. Catal.* **1998**, *117*, 13.
(7) Kelleher, B. P.; O'Dwyer, T. F.; Doyle, A. M.; Hodnett, B. K. *J. Chem. Technol. Biotechnol.* **2001**, *76*, 1216.
(8) Han, Y.-J.; Stucky, G. D.; Butler, A. *J. Am. Chem. Soc.* **1999**, *121*, 9897.
(9) Wang, J. *Anal. Chim. Acta*. **1999**, *399*, 21.
(10) Wang, B.; Zhang, J.; Cheng, G.; Dong, S. *Anal. Chim. Acta*. **2000**, *407*, 111.
(11) Gill, I. and Ballesteros, A. *J. Am. Chem. Soc.* **1998**, *120*, 8587.
(12) Washmon-Kriel, L.; Jimenez, V. L.; Balkus, K. J., Jr. *J. Mol. Catal. B: Enz.* **2000**, *10*, 453.
(13) Deere, J.; Magner, E.; Wall, J. G.; Hodnett, B. K. *Chem. Commun.* **2001**, 465.
(14) Weetall, H. H. *App. Biochem. Biotech*. **1993**, *41*, 157.
(15) Docoslis, A.; Wu, W.; Giese, R. F.; Van Oss, C. J. *Coll. and Surf. B: Biointerfaces*. **1999**, *13*, 83.
(16) Malmsten M. *J. Coll. Int. Sci.* **1994**, *166*, 333.
(17) Jönsson, U.; Ivarsson, B.; Lundström, I.; Berghem, L. *J. Coll. Inter. Sci.* **1982**, *90*, 148.
(18) Weetall, H. H. *Science*. **1969**, *166*, 615.
(19) Weetall, H. H. *Met. Enzymol*. **1976**, *44*, 134
(20) Weetall, H. H.; Vann, W. P.; Pitcher, W. H.; Lee, D. D.; Lee, Y. Y.; Tsao, G. T. *Met. Enzymol*. **1976**, *44*, 776.
(21) Weetall, H. H. and Vann, W. P. *Biotech. Bioeng*. **1976**, *18*, 105.
(22) Weetall, H. H. *Anal. Chem.* **1974**, *46*, 602.
(23) Weetall, H. H. *Analytical Uses of Immobilised Biological Compounds for Detection, Medical and Industrial Uses*; Guilbault, G. G., Mascini, M., Eds.: D. Reidel Publishing Co.: Boston, MA, 1988; 1.
(24) Diaz, J. F.; Balkus, K. J., Jr. *J. Mol. Catal. B: Enz*. **1996**, *2*, 115.
(25) He, J.; Li, X.; Evans, D. G.; Duan, X.; Li, C. *J. Mol. Catal. B: Enz*. **2000**, *11*, 45.
(26) Kisler, J. M.; Dähler, A.; Stevens, G. W.; O'Connor, A. J. *Micro. Meso. Mat*. **2001**, *44*−*45*, 769.
(27) Yiu, H. H. P.; Wright, P. A.; Botting, N. P. *Micro. Meso. Mat*. **2001**, *44*−*45*, 763.
(28) Yiu, H. H. P.; Wright, P. A.; Botting, N. P. *J. Mol. Catal. B: Enz*. **2001**, *15*, 81.
(29) Takahashi, H.; Li, B.; Sasaki, T.; Miyazaki, C.; Kajino, T.; Inagaki, S. *Micro. Meso. Mat*. **2001**, *44*−*45*, 755.
(30) Han, Y.-J.; Watson, J. T.; Stucky, G. D.; Butler, A. *J. Mol. Catal. B: Enz*. **2001**, *671*, 1.
(31) Scott, R. A.; Mauk, A. G. *Cytochrome c, A Multidisciplinary Approach*; University Science Books: Sausalito, California, 1996.
(32) Bushnell, G. W.; Louie, G. V.; Brayer, G. V. *J. Mol. Biol.* **1990**, *1990*, 585.
(33) Moore, G. R. and Pettigrew, G. W. *Cytochrome c*: *Evolutionary, Structural and Physicochemical Aspects*; Springer-Verlag: Berlin, 1990.
(34) Spiro, T. G. *Biological Applications of Raman Spectroscopy*; John Wiley and Sons: New York, 1998.
(35) Hildebrandt, P.; Heimburg, T.; Marsh, D.; Powell G. L. *Biochemistry* **1990**, *29*, 1661.
(36) Choi, S. and Spiro, T. G. *J. Am. Chem. Soc.* **1983**, *105*, 3683.
(37) Hildebrandt, P. and Stockburger, M. *J. Phys. Chem.* **1986**, *90*, 6017.
(38) Margoliash, E. and Lustgarten, J. *J. Biol. Chem.* **1962**, *237*, 3397.
(39) Zhao, D.; Huo, Q.; Feng, J.; Chmelka, B. F.; Stucky, G. D. *J. Am. Chem. Soc.* **1998**, *120*, 6024.
(40) Barrett, E. P.; Joyner, L. G.; Halenda, P. P. *J. Am. Chem. Soc.* **1951**, *73*, 373.
(41) Brunauer, S.; Emmett, P. H.; Teller, E. *J. Am. Chem. Soc.* **1938**, *60*, 309.
(42) Walsh, K. and Neurath, H. *Proc. Natl. Acad. Sci. U.S.A.* **1964**, *52*, 884.
(43) Markland, F. S. and Smith, E. L. *The Enzymes*; Academic Press: London, 1976.
(44) Swoboda, B. E. P. and Massey, V. *J. Biol. Chem.* **1965**, *240*, 2209.
(45) Bhattacharyya, J.; Bhattacharyya, M.; Chakraborti, A. S.; Choudhuri, U.; Poddar, R. K. *Int. J. Biol. Macromol*. **1998**, *23*, 11.
(46) Braun, S.; Shtelzer, S.; Rappoport, S.; Avnir, D.; Ottolenghi, M. *J. Non-Cryst. Sol*. **1992**, *147*−*148*, 739.
(47) Elgersma, A. V.; Zsom, R. L. J.; Norde, W.; Lyklema, J. *J. Coll. Inter. Sci.* **1990**, *138*, 145.
(48) Gimon-Kinsel, M. E.; Jimenez, V. L.; Washmon, L.; Balkus, K. J., Jr. *Mesoporous Molecular Sieves, Studies in Surface Science and Catalysis*; Elsevier: Amsterdam, 1998.
(49) Parks, G. A. *Chem. Rev*. **1965**, *65*, 177.
(50) Antonini, E.; Brunori, M. *Hemoglobin and myoglobin in their reaction with ligands*; North-Holland, Amsterdam-London, 1976.
(51) Weber, G.; Young, L. B. *J. Biol. Chem.* **1964**, *239*, 1424.
(52) Bovey, F.; Yanari, S. *The Enzymes*; Vol. IV Academic Press: London, 1960.
(53) Bourdillon, C.; Bourgeois, J. P.; Thomas, D. *J. Am. Chem. Soc.* **1980**, *102*, 4231.
(54) Ahmad, A.; Akhtar, Md. S.; Bhakuni, V. *Biochemistry* **2001**, *40*, 1945.
(55) Smulevich, G.; Spiro, T. G. *J. Phys. Chem.* **1985**, *89*, 5168.
(56) Li, X.-Y.; Czernuszewicz, R. S.; Kincaid, J. R.; Spiro, T. G. *J. Am. Chem. Soc*. **1989**, *111*, 7012.
(57) Li, X.-Y.; Czernuszewicz, R. S.; Kincaid, J. R.; Su, Y. O.; Spiro, T. G. *J. Phys. Chem.* **1990**, *94*, 31.
(58) Czernuszewicz, R. S.; Li, X.-Y.; Spiro, T. G. *J. Am. Chem. Soc.* **1989**, *111*, 7024.
(59) Vincent, J. S.; Levin, I. W. *J. Am. Chem. Soc.* **1986**, *108*, 3551.
(60) Cotton, T. M.; Schultz, S. G.; Van Duyne, R. P. *J. Am. Chem. Soc.* **1980**, *102*, 7960.
(61) Choi, S.; Lee, J. J.; Wei Y. H.; Spiro, T. G. *J. Am. Chem. Soc.* **1983**, *105*, 3692.
(62) Valance, W. G.; Strekas, T. C. *J. Phys. Chem.* **1982**, *86*, 1804.
(63) Griebenow, K.; Klibanov, A. M. *J. Am. Chem. Soc.* **1996**, *118*, 11696.
(64) Ångström, J.; Moore, G. R.; Williams, R. J. P. *Biochim. Biophys. Acta*. **1982**, *703*, 87.
(65) Spiro, T. G. and Strekas, T. C. *Proc. Natl. Acad. Sci. U.S.A.* **1972**, *69*, 2622.